1521-009X/49/6/442–450$35.00
DRUG METABOLISM AND DISPOSITION

https://doi.org/10.1124/dmd.121.000356
Drug Metab Dispos 49:442–450, June 2021

Cytochrome P450 3A Time-Dependent Inhibition Assays Are Too Sensitive for Identification of Drugs Causing Clinically Significant Drug-Drug Interactions: A Comparison of Human Liver Microsomes and Hepatocytes and Definition of Boundaries for Inactivation Rate Constants[S]

Heather Eng, Elaine Tseng, Matthew A. Cerny, Theunis C. Goosen, and R. Scott Obach

Medicine Design, Pfizer Inc., Groton, Connecticut

Received January 1, 2021; accepted March 18, 2021

ABSTRACT

Time-dependent inhibition (TDI) of CYP3A is an important mechanism underlying numerous drug-drug interactions (DDIs), and assays to measure this are done to support early drug research efforts. However, measuring TDI of CYP3A in human liver microsomes (HLMs) frequently yields overestimations of clinical DDIs and thus can lead to the erroneous elimination of many viable drug candidates from further development. In this investigation, 50 drugs were evaluated for TDI in HLMs and suspended human hepatocytes (HHEPs) to define appropriate boundary lines for the TDI parameter rate constant for inhibition (k_{obs}) at a concentration of 30 μM. In HLMs, a k_{obs} value of 0.002 minute^{-1} was statistically distinguishable from control; however, many drugs show k_{obs} greater than this but do not cause DDI. A boundary line defined by the drug with the lowest k_{obs} that causes a DDI (diltiazem) was established at 0.01 minute^{-1}. Even with this boundary, of the 33 drugs above this value, only 61% cause a DDI (true positive rate). A corresponding analysis was done using HHEPs; k_{obs} of 0.0015 minute^{-1} was statistically distinguishable from control, and the boundary was established at 0.006 minute^{-1}. Values of k_{obs} in HHEPs were almost always lower than those in HLMs. These findings offer a practical guide to the use of TDI data for CYP3A in early drug-discovery research.

SIGNIFICANCE STATEMENT

Time-dependent inhibition of CYP3A is responsible for many drug interactions. In vitro assays are employed in early drug research to identify and remove CYP3A time-dependent inhibitors from further consideration. This analysis demonstrates suitable boundaries for inactivation rates to better delineate drug candidates for their potential to cause clinically significant drug interactions.

Introduction

CYP3A is the major drug-metabolizing enzyme in humans and is expressed in the liver and intestine. It contributes to the metabolic clearance and first-pass extraction of a vast array of drugs and, as such, is also the target for numerous pharmacokinetic drug-drug interactions (DDIs). Interactions arise via coadministration of CYP3A-cleared drugs with those that cause inhibition (e.g., itraconazole), inactivation (e.g., clarithromycin), or induction (e.g., rifampin) of the enzyme. Depending on the rate and fraction of clearance and/or first-pass extraction occurring via CYP3A-mediated metabolism, the magnitude of drug interactions can be high. For example, the antianxiety agent buspirone, which has high clearance and a high fraction of its metabolism catalyzed by CYP3A, has been reported to have increases in exposure of up to 19-fold with coadministration of itraconazole (Kivistö et al., 1997). Time-dependent inactivators (TDIs) also elicit significant DDIs when coadministered with the sensitive CYP3A marker substrate midazolam (e.g., ritonavir increased midazolam exposure 26-fold) (Greenblatt et al., 2009). Moreover, combination therapy with ritonavir and indinavir (not a known TDI) increased alfentanil exposure 37-fold (Kharasch et al., 2009).

Over the past 2 decades, considerable effort has been made to develop in vitro assays for cytochrome P450 activity that can be used to evaluate drugs and other xenobiotics as inhibitors and time-dependent inactivators of this important enzyme. Complex assays to measure K_I and k_{inact} are used in drug development, and these parameters can be used in combination with other input values to make estimates of DDI using mechanistic and physiologically based pharmacokinetic modeling. Such data can also be used in calculating the "R2" value described by the US Food and Drug Administration to make a first decision regarding whether a new drug candidate needs further evaluation (Food and Drug Administration, 2020). In earlier phases of drug research, assays to measure TDI that are pared down from the labor-intensive full determination of K_I and k_{inact} have been described, such as the IC_{50} shift or 2 + 2 assays (Grimm et al., 2009). Midazolam 1′-hydroxylase and testosterone 6β-hydroxylase activities have been most frequently employed as marker activities for CYP3A4 (and the closely related enzyme CYP3A5 for midazolam) in human liver microsomal (HLM)

This work received no external funding.
Declaration of interest: The authors report no conflicts of interest. The authors alone are responsible for the content and writing of the paper.
https://doi.org/10.1124/dmd.121.000356.
[S] This article has supplemental material available at dmd.aspetjournals.org.

ABBREVIATIONS: AUCR, area-under-the-plasma-concentration-time-curve ratio; DDI, drug-drug interaction; HHEP, human hepatocyte; HLM, human liver microsome; K_I, inhibition constant; k_{inact}, maximal rate of enzyme inactivation; k_{obs}, rate constant for inactivation; LC-MS/MS, tandem liquid chromatography–mass spectrometry; TDI, time-dependent inhibition.

preparations (Kawano et al., 1987; Waxman et al., 1988; Gorski et al., 1994; Kokudai et al., 2009). Data obtained from such assays can be combined with other input parameters (in vivo concentration of the inhibitor, fraction of the substrate that is cleared by CYP3A in vivo) and used to make comparisons among compounds and predictions of the magnitude of DDI in vivo. Methods used to correlate in vitro inhibition data to in vivo DDI range from the use of simple relationships derived from the Rowland-Matin equation (Rowland and Matin, 1973) to more sophisticated physiologically based pharmacokinetic modeling approaches (Jones and Rowland Yeo, 2013).

Because of the high number of drugs cleared by CYP3A-mediated metabolism, in vitro assays to measure inhibition of this enzyme are frequently employed early in the drug research process to avoid developing new drugs that could cause DDI with CYP3A-cleared drugs. The data from these assays can be used in a simple screening-type strategy (i.e., qualitatively categorizing as an inhibitor versus noninhibitor) or in developing structure-activity relationships that can be used in designing away from CYP3A inhibition. As drug research projects approach the selection of the best candidate compound to bring forth into the development phase, in vitro CYP3A inhibition data are used in the prediction of DDI when combined with other important input parameters, such as dose, free fraction in plasma, and projected clinical exposure. Assays used include tests for simple reversible inhibition as well as time-dependent irreversible inactivation. Reversible inhibition data for CYP3A have been generally found to be reliable in the prediction of DDI (Obach et al., 2006; Einolf, 2007; Vieira et al., 2014); however, time-dependent inhibition frequently overestimates the magnitude of DDI (Obach et al., 2007; Kenny et al., 2012; Vieira et al., 2014). The reasons for overprediction for TDI are not known.

Time-dependent inhibition of cytochrome P450 enzymes can occur via a few different mechanisms. Metabolism of certain chemical substituents (e.g., alkylamines, methylenedioxyphenyl) can yield intermediate metabolites that can form a tight noncovalent interaction with the heme iron [referred to as metabolite-intermediate complex formation (Franklin, 1977)]. Examples of drugs that inactivate CYP3A by this mechanism include verapamil, lapatinib, and erythromycin (McConn et al., 2004; Wang et al., 2005; Barbara et al., 2013). Metabolism of other chemical substituents can lead to the generation of reactive electrophilic intermediates that can form covalent bonds with the enzyme or the heme. Drugs that inactivate CYP3A in this manner include ethinyl estradiol, raloxifene, and ritonavir (Lin et al., 2002; Baer et al., 2007; Rock et al., 2014). For these mechanisms of inactivation, the relationship between chemical structure, metabolism/bioactivation, and inactivation is well understood. However, in the routine employment of a liver microsomal CYP3A time-dependent inhibition screening assay in early drug discovery [i.e., measurement of inactivation rate constant (k_{obs}) at a test concentration of 30 μM], we have found that 75% (unpublished observations) of new compounds synthesized exhibited time-dependent inhibition. An observation similar to this was reported by Zimmerlin et al. (2011) using a test concentration of 10 μM. The vast majority of compounds showing k_{obs} values that are statistically different from solvent control possess no obvious chemical structure associated with the aforementioned inactivation mechanisms. Thus, drug-discovery project teams are faced with the dilemma of whether the assay findings for a compound of interest truly portend a DDI risk, which will require further design efforts to mitigate that risk, or whether the assay is either oversensitive or generates artifactual findings for the compound. One hypothesis for this is whether liver microsomes artificially lack some unknown factor present in vivo that protects against the inactivation of CYP3A. Early efforts we made to address this by adding factors, such as ascorbate, superoxide dismutase, glutathione, and other agents, to microsomal TDI assays had no impact on reducing TDI rates (unpublished observations).

The use of suspended human hepatocytes (HHEPs) as an alternate system to measure CYP3A TDI has been proposed because they are more physiologically relevant than HLMs. HHEPs have an intact cell membrane, a full complement of drug-metabolizing enzymes, and physiologic cofactor concentrations. Chen et al. (2011) compared inactivation kinetics for four CYP3A TDIs and showed that K_I was greater in hepatocytes than in microsomes with k_{inact} mostly unchanged. Conversely, some authors have shown comparable K_I values, whereas HHEP k_{inact} was significantly reduced relative to that of HLMs (Mao et al., 2013; Kimoto et al., 2019). More recently, it has been suggested that HLM inactivation parameters corrected for free cytosolic inhibitor concentrations estimated in HHEPs could improve DDI predictions (Filppula et al., 2019). Mao and coworkers (2011, 2012, 2016) have evaluated HHEPs as a system for measuring TDI, also adding plasma to the incubation medium to include the impact of protein binding on projection of in vivo DDI with improved success.

Based on our experiences with overprojection of DDI from liver microsomal TDI data and the high rates of positive TDI without obvious structural alerts among thousands of new chemical entities in drug-discovery programs, we endeavored to make a systematic comparison of liver microsomes and suspended HHEPs for CYP3A TDI. Fifty drugs for which clinical DDI data for CYP3A exist (both positive and negative) were evaluated for TDI in liver microsomes and hepatocytes. The overall objectives were 1) to compare TDI kinetics in the two systems to determine whether there is a systematic trend of higher inactivation in microsomes and 2) to develop an empirically driven cutoff value for k_{obs} (at [I] = 30 μM) under which drug design teams can be more assured that DDI will not be a clinical problem.

Materials and Methods

Materials. Research was conducted on human tissue acquired from a third party that has been verified as compliant with Pfizer policies, including institutional review board/independent ethic committee approval. Human liver microsomes pooled from 36 male and 14 female donors were purchased from Sekisui XenoTech (Kansas City, KS). Cryopreserved HHEPs pooled from four male and six female donors were purchased from BioIVT (Westbury, NY). Monobasic and dibasic potassium phosphate buffers, magnesium chloride, NADPH, HEPES, and DMSO were purchased from Sigma (St. Louis, MO). Midazolam was purchased from U.S. Pharmacopeia (Rockville, MD). 1′-Hydroxymidazolam and [$^2H_4$]-1′-hydroxymidazolam were synthesized at Pfizer (Groton, CT). William's medium E was purchased from Gibco (Dublin, Ireland). Commercially obtained chemicals and solvents were of high-performance liquid chromatography or analytical grade. Tested drugs were purchased from one of the following sources: Sigma-Aldrich, Toronto Research Chemicals (North York, ON, Canada), or MedChemExpress (Monmouth Junction, NJ).

Identification of Test Drugs. A list of drugs for which clinical CYP3A interaction studies have been conducted was compiled using the University of Washington Drug Interaction Database (https://www.druginteractionsolutions.org). For drugs in which more than one interaction study was published, the study that had the greatest magnitude of interaction was selected. Oral midazolam was the preferred probe substrate, but in a few cases, studies using intravenous midazolam or alternate CYP3A probe substrates were referenced. The magnitude of DDI was based on area-under-the-plasma-concentration-time-curve ratios (AUCRs).

Time-Dependent Inhibition in Human Liver Microsomes. Time-dependent inhibition of CYP3A was measured in human liver microsomes (0.3 mg/ml) supplemented with $MgCl_2$ (3.3 mM) and NADPH (1.3 mM) in potassium phosphate buffer (100 mM, pH 7.4). Drug stock solutions prepared at 100 times the incubation concentration in 50% acetonitrile and 50% water, or control solvent was added to this incubation mixture to initiate the reaction. Final incubation concentration was typically 30 μM. At various time points (1, 5, 10, 20, 30, and 40 minutes), an aliquot of this mixture was transferred to an activity incubation

mixture containing midazolam (20.9 μM, 10-fold K_M), $MgCl_2$ (3.3 mM), and NADPH (1.3 mM) in potassium phosphate buffer (100 mM, pH 7.4), resulting in a 20-fold dilution. After 6 minutes, the activity reaction was terminated by the addition of two volumes of acetonitrile containing internal standard (100 ng/ml [$^2H_4$]-1′-hydroxymidazolam). All reactions were carried out at 37°C at a final volume of 200 μl and done in duplicate. Samples were vortexed and centrifuged for 5 minutes at approximately 2300*g* at room temperature. The supernatant was mixed with an equal volume of water containing 0.2% formic acid and analyzed directly by tandem liquid chromatography–mass spectrometry (LC-MS/MS).

For several drugs, assay conditions had to be modified to accommodate potent inhibition at the initial time point and rapid inactivation. A 50-fold dilution was used for mibefradil, propiverine, saquinavir, and simvastatin. Lower concentrations were tested: 1 μM for itraconazole; 3 μM for cobicistat, conivaptan, mibefradil, nelfinavir, and tofisopam; and 10 μM for nilotinib. An alternate stock solvent was used to prepare clarithromycin (6% DMSO, 94% acetonitrile), nefazodone (20% DMSO, 80% acetonitrile), pimavanserin (6% DMSO, 20% water, 74% acetonitrile), ritonavir (64% acetonitrile, 36% water), sorafenib (90% ethanol, 10% water), terbinafine (44% acetonitrile, 16% methanol, 40% water), terfenadine (65% acetonitrile, 15% methanol, 17% water), alectinib (12% DMSO, 42% acetonitrile, 38% methanol, 8% water), carfilzomib (11% DMSO, 22% water, 67% acetonitrile), midostaurin (9% DMSO, 74% acetonitrile, 17% water), and telaprevir (10% DMSO, 49% acetonitrile, 20.5% methanol, 20.5% water). The final total solvent in the primary incubations was ≤1%.

Time-Dependent Inhibition in Suspension Human Hepatocytes. Time-dependent inhibition of CYP3A was measured in HHEPs (0.45 million hepatocytes/ml) suspended in William's medium E supplemented with L-glutamine and HEPES (50 mM). Drug stock solutions prepared at 10 times the incubation concentration in 90% media, 5% acetonitrile, and 5% water were added to this incubation mixture to initiate the reaction. The final incubation concentration was typically 30 μM (unless otherwise stated) in a volume of 50 μl. At various time points (typically 5, 10, 30, 60, 90, and 120 minutes unless otherwise stated), a 200-μl aliquot of the activity incubation mixture consisting of midazolam (final concentration 80 μM, approximately 5-fold K_M) in media was added to the incubation wells, resulting in a 5-fold dilution. After 20 minutes (which had previously been demonstrated to show linear product formation with time), the activity reaction was terminated by the addition of two volumes of acetonitrile containing internal standard (100 ng/ml [$^2H_4$]-1′-hydroxymidazolam). All reactions were carried out at 37°C in a humidified incubator (75% relative humidity, 5% CO_2) in duplicate. Samples were vortexed and centrifuged for 5 minutes at approximately 2300*g* at room temperature. The supernatant was mixed with an equal volume of water containing 0.2% formic acid and analyzed directly by LC-MS/MS.

For several drugs, the assay conditions had to be modified to accommodate potent inhibition observed at the initial time point, rapid inactivation, or insolubility. Drugs with shortened primary incubation times (3, 5, 10, 15, 20, and 30 minutes) due to rapid inactivation include troleandomycin, tabimorelin, telithromycin, boceprevir, erythromycin, amlodipine, imatinib, saquinavir, cobicistat (3 μM), conivaptan (3 μM), nelfinavir (3 μM), and mibefradil (3 μM). The drugs with solubility issues when prepared in media required dilution directly from organic stocks (prepared at 100 times the final incubation concentration) into suspension hepatocytes: simvastatin, alectinib, carfilzomib, midostaurin, sorafenib, tadalafil, and mibefradil (3 μM); these drugs were tested at a final density of 0.5 million hepatocytes/ml.

LC-MS/MS Methodology for the Quantitation of 1′-Hydroxymidazolam. LC-MS/MS analysis was conducted on a Sciex 6500 triple quadrupole mass spectrometer (Framingham, MA) fitted with an electrospray ion source operated in positive ion mode using multiple reaction monitoring. An Agilent 1290 binary pump (Santa Clara, CA) with a CTC Leap autosampler (Leap Technology, Carrboro, NC) was programmed to inject 10 μl of sample on a Halo 2.7 μm C18 2.1 × 30 mm column (Advanced Materials Technology, Wilmington, DE). A binary gradient was employed using 0.1% (v/v) formic acid in water (mobile phase A) and 0.1% (v/v) formic acid in acetonitrile (mobile phase B) at a flow rate of 0.5 ml/min. Mass-to-charge transitions for analytes 1′-hydroxymidazolam and [$^2H_4$]-1′-hydroxymidazolam were 342.2 → 324.2 and 346.2 → 328.2, respectively. Analytes were quantified using Analyst software (Sciex). The peak area ratio of analyte to internal standard was used to determine inactivation rates.

Estimation of Observed Inactivation Rate. Data analysis methods have been previously described (Yates et al., 2012). Briefly, k_{obs} was determined by normalizing the peak area ratio in each sample to that of the mean solvent control area ratio in the initial time point, plotting the natural log of percent remaining activity versus preincubation time, and then calculating the slope of the line ($-k_{obs}$) using the initial linear portion of the curve. A statistical test was done for each drug to determine whether k_{obs} was statistically different from the within-experiment solvent control (i.e., a parallel lines test), as shown in eq. 1.

$$z = \frac{\left|k_{obs[I]} - k_{obs[0\mu M]}\right|}{\sqrt{S.E._{k_{obs[I]}}^{2} + S.E._{k_{obs[0\mu M]}}^{2}}} \quad (1)$$

Here $k_{obs[I]}$ and $k_{obs[0\mu M]}$ represent the inactivation rate for an inhibitor at a single concentration and inactivation rate with solvent control, respectively. When $P < 0.05$, there is statistically significant or measurable TDI. Analyses were performed using Microsoft Excel (Redmond, WA) and GraphPad Prism (La Jolla, CA). To account for between-assay variability, k_{obs} of the within-experiment solvent control was subtracted from each drug k_{obs}. (In hepatocytes, any subsequent formation of glucuronide conjugates of 1′-hydroxymidazolam was not measured but would be expected to be formed at small levels, and furthermore, k_{obs} values are calculated relative to the solvent control in which this secondary metabolism would also be occurring.)

Confusion Matrix Analyses. This analysis was done separately for the HLM and HHEP results. True positives were defined as compounds that were above the k_{obs} boundary line and had an observed AUCR ≥2. True negatives were compounds that were below the k_{obs} boundary line and had an observed AUCR <2. False positives were compounds that were above the k_{obs} boundary line but did not exhibit DDI (AUCR < 2), whereas false negatives were below the k_{obs} boundary line and did exhibit DDI (AUCR ≥ 2). The boundary line was set at the lowest k_{obs} associated with a clinical DDI of >2-fold. Positive predictive value describes the chance of an in vitro positive result exhibiting a clinical DDI (eq. 2).

$$Positive\ predictive\ value = 100 \times \frac{True\ positive}{True\ positive + False\ positive} \quad (2)$$

The analysis was repeated, but rather than using the k_{obs} boundary line, the parallel lines test k_{obs} P value was used to define the in vitro TDI positives ($P < 0.05$) and negatives ($P \geq 0.05$).

Results

Clinical drug interactions (AUCRs) for CYP3A DDI studies for 50 drugs are summarized in Table 1. The majority of studies (43) used midazolam as the CYP3A substrate, whereas the remaining studies employed alprazolam (1), triazolam (2), simvastatin (2), terfenadine (1), or buspirone (1). Of the drugs listed in Table 1, 26 drugs have no clinical drug-drug interaction (AUCR < 1.25), 4 have weak interactions (AUCR 1.25–2), and 20 have moderate [AUCR 2–5 (6)] or strong [AUCR > 5 (14)] interactions.

Representative examples of plots of natural log of percent activity remaining versus time determined in HLMs are presented in Fig. 1. These plots show CYP3A activity lost over time for NADPH-supplemented incubations containing solvent (solvent control), a drug that is statistically different from solvent control (eplerenone), a moderate inactivator (imatinib), and a fast inactivator (disulfiram). For most drugs, a 30 μM test concentration was used. However, lower concentrations were used for some drugs because of limits on aqueous solubility, potent reversible inhibition, or rapid time-dependent inhibition. A summary of k_{obs} determined in HLMs and HHEPs are presented in Supplemental Table 1 and Table 2. Rates of inactivation (solvent control–corrected) from the HLM assay ranged from −0.001 (terbinafine) to 0.2333 minute^{-1} (0.3 μM ritonavir). By comparison, the average HLM solvent control k_{obs} value was found to be 0.0056 ± 0.0014 minute^{-1} (S.D.). HHEP k_{obs} values ranged from −0.0003 (citalopram, flumazenil) to 0.2826

TABLE 1

Observed maximal clinical drug-drug interactions for well established CYP3A cleared drugs

Drug Name	Dose	Victim	Clinical Interaction (AUCR)	Clinical Interaction Reference
Erlotinib	150 mg QD; 14 days	7.5 mg PO midazolam	0.67	Calvert et al. (2014)
Terbinafine	250 mg QD, 4 days	7.5 mg PO midazolam	0.75	Ahonen et al. (1995)
Alectinib	600 mg BID, 21 days	2 mg PO midazolam	0.84	Morcos et al. (2017)
Sorafenib	400 mg BID, 28 days	2 mg PO midazolam	0.85	Flaherty et al. (2011)
Pimavanserin	Not provided, 38 days	Midazolam (dose not provided)	0.86	Food and Drug Administration (2016)
Fluoxetine	20 mg QD; 7 days	10 mg PO midazolam	0.87	Lam et al. (2003)
Propranolol	40 mg QID, 2 days	0.5 mg PO triazolam	0.89	Friedman et al. (1988)
Tadalafil	10 mg QD, 14 days	15 mg PO midazolam	0.9	Ring et al. (2005)
Nitrendipine	20 mg single dose	0.07 mg/kg i.v. plus infusion midazolam	0.93 change in CL	Handel et al. (1988)
Citalopram	40 mg QD; 30 days	0.25 mg PO triazolam	0.94	Nolting and Abramowitz (2000)
Ramelteon	32 mg QD, 10 days	10 mg PO midazolam	0.94	Food and Drug Administration (2005a)
Eplerenone	100 mg QD; 6 days	10 mg PO midazolam	0.96	Cook et al. (2004)
Paroxetine	20 mg QD; 15 days	60 mg PO terfenadine	0.97	Martin et al. (1997)
Flumazenil	0.5 mg, single dose	0.03 mg/kg i.v. midazolam	0.98	Raeder et al. (1988); Rogers et al. (2002)
Naltrexone	50 mg QD; 14 days	2 mg PO midazolam	0.98	Adams et al. (2005)
Midostaurin	100 mg, single dose	4 mg PO midazolam	1	Dutreix et al. (2013)
Quetiapine	1467 mg/day	0.075 mg PO midazolam	1 (no interaction, midazolam metabolic ratio)	Khazaal et al. (2013)
Panobinostat	20 mg every other day; 15 days	5 mg PO midazolam	1.04	Einolf et al. (2017)
Disulfiram	500 mg, single	1 mg i.v. midazolam	1.05	Kharasch et al. (1999)
Buspirone	10 mg TID; 7 days	1 mg PO alprazolam	1.08	Buch et al. (1993)
Atomoxetine	60 mg BID; 12 days	5 mg PO midazolam	1.09	Sauer et al. (2004)
Raltegravir	400 mg BID, 14 days	2 mg PO midazolam	1.09	Iwamoto et al. (2008)
Carfilzomib	27 mg/m^2, i.v., various	2 mg PO midazolam	1.1	Wang et al. (2013)
Terfenadine	120 mg QD, 3 days	10 mg PO buspirone	1.19	Lamberg et al. (1999)
Ethinyl estradiol	0.035 mg QD, 10 days	7.5 mg PO midazolam	1.2	Palovaara et al. (2000)
Simvastatin	10 mg QD, 14 days	15 μg/kg PO midazolam	1.24	Kokudai et al. (2009)
Azithromycin	500 mg QD; 3 days	15 mg PO midazolam	1.27	Zimmermann et al. (1996)
Propiverine	15 mg BID, 15 days	2 mg PO midazolam	1.46	Tomalik-Scharte et al. (2005)
Amlodipine	400 mg QD, 4 days	40 mg PO simvastatin	1.75	Becquemont et al. (2007)
Tabimorelin	2.86–3.21 mg PO, 7 days	7.5 mg PO midazolam	1.93	Zdravkovic et al. (2003)
Tofisopam	100 mg TID, 9 days	7.5 mg PO midazolam	2.36	Tóth et al. (2008)
Nilotinib	400 mg BID, 12 days	2 mg PO midazolam	2.40	Zhang et al. (2015)
Imatinib	400 mg QD, 7 days	40 mg PO simvastatin	2.92	O'Brien et al. (2003)
Verapamil	80 mg TID, 2 days	15 mg PO midazolam	2.92	Backman et al. (1994)
Diltiazem	60 mg TID; 2 days	2 mg PO midazolam	4.06	Friedman et al. (2011)
Erythromycin	1000 mg	3 μg PO midazolam	4.99	Carls et al. (2014)
Boceprevir	800 mg TID, 6 days	4 mg PO midazolam	5.05	Food and Drug Administration (2011)
Idelalisib	150 mg BID, 10 days	5 mg PO midazolam	5.15	Jin et al. (2015)
Saquinavir	1200 mg TID, 5 days	7.5 mg PO midazolam	5.18	Palkama et al. (1999)
Nelfinavir	1250 BID, 14 days	2 mg PO midazolam	5.29	Kirby et al. (2011)
Nefazodone	200 mg BID; 7 days	10 mg PO midazolam	5.44	Lam et al. (2003)
Conivaptan	40 mg BID, 5 days	2 mg PO midazolam	5.76	Food and Drug Administration (2005b)
Telithromycin	800 mg QD, 6 days	6 mg PO midazolam	6.2	Food and Drug Administration (2004)
Mibefradil	100 mg, single dose	2 mg PO midazolam	8.86	Veronese et al. (2003)
Clarithromycin	500 mg BID; 7 days	4 mg PO midazolam	9.61	Gorski et al. (1998)
Itraconazole	200 mg QD, 4 days	7.5 mg PO midazolam	10.77	Olkkola et al. (1994)
Telaprevir	750 mg TID, 16 days	2 mg PO midazolam	13.5	Garg et al. (2012)
Troleandomycin	500 mg	3 mg PO midazolam	14.83	Kharasch et al. (2004)
Cobicistat	200 mg PO, 14 days	5 mg PO midazolam	19.03	Mathias et al. (2010)
Ritonavir	100 mg BID, 2 days	3 mg PO midazolam	26.41	Greenblatt et al. (2009)

BID, twice daily; PO, by mouth; QD, once daily; QID, four times a day; TID, three times daily.

minute^{-1} (troleandomycin). By comparison, the average HHEP solvent control k_{obs} value was found to be -0.0010 ± 0.0030 minute^{-1} (S.D.). It should be noted that the solvent control k_{obs} value for HLM was measurable, whereas the solvent control k_{obs} in HHEP was essentially zero Fig. 2.

In general, drugs exhibit lower k_{obs} values in the HHEP assay compared with that of HLM. Plots of HHEP versus HLM k_{obs} for the 43 drugs determined in both systems at the same concentration are presented in Fig. 3. No apparent correlation is observed in the linear-scaled plot (Fig. 3A). However, for the vast majority of drugs, the HLM k_{obs} was markedly higher than the HHEP k_{obs}. A log-scaled plot (Fig. 3B) shows this trend. In contrast, three drugs—troleandomycin, saquinavir, and cobicistat—appear to have significantly higher HHEP k_{obs} compared with their HLM k_{obs} values.

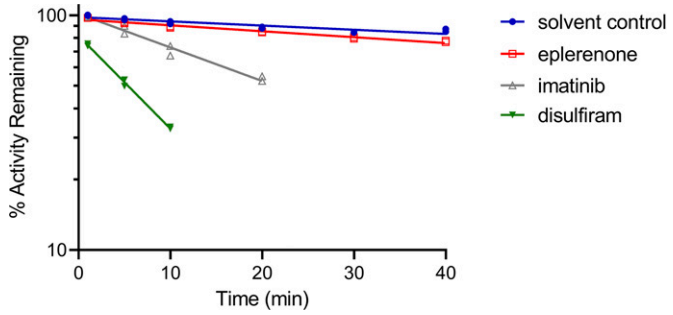

Fig. 1. Plot of representative HLM percent activity remaining data. The percent remaining activity is shown along with a regression in which the slope represents $-k_{obs}$. This illustrates a representative k_{obs} from a solvent control (0.0040 minute^{-1}), a drug that is statistically different from the solvent control yet registers below the DDI boundary (eplerenone, 0.0058 minute^{-1}), a moderate inactivator (imatinib, 0.0235 minute^{-1}), and a faster inactivator (disulfiram, 0.0865 minute^{-1}). These studies were conducted $n = 2$.

A total of 50 drugs were evaluated for CYP3A TDI in HLMs and ranked in order of increasing k_{obs} in Fig. 4A. Arranging the data from low to high, diltiazem (k_{obs} of 0.011 minute^{-1}) is the first drug for which a clinical DDI magnitude exceeds the 2-fold boundary line. A boundary line corresponding to the k_{obs} of 0.01 minute^{-1} is established, above which a 2-fold clinical interaction is more likely. Similarly, Fig. 4B shows data for 44 drugs evaluated for CYP3A in the HHEP TDI assay. A boundary of 0.006 minute^{-1} for the HHEPs is proposed. The drug with the lowest k_{obs} value at 30 μM that shows a 2-fold DDI in vivo is diltiazem, and thus a boundary for k_{obs} set from that drug would be 0.006 minute^{-1}. (It should be noted mibefradil, which yielded a k_{obs} of 0.0045 minute^{-1}, had to be tested at 0.3 μM and not the standard 30 μM concentration used for other drugs because inactivation was too rapid to be accurately measured at the 100-fold higher concentration. At 30 μM, mibefradil would have shown a k_{obs} much greater than the 0.006 minute^{-1} cutoff.) Diltiazem serving as the boundary would be consistent for both in vitro systems. The data were further evaluated in a confusion matrix for sensitivity and specificity of these assays (Fig. 5). For DDI, a binary categorization for DDI is defined by a boundary of 2-fold, which for making decisions early in the drug design process is deemed adequate, as opposed to the strict bioequivalence cutoff values for DDI used in drug regulatory definitions (see explanation in the *Discussion* below). For the in vitro data, two different criteria for cutoffs were evaluated: (a) k_{obs} values deemed statistically different from solvent control (by $P < 0.05$) and (b) the aforementioned cutoff values for k_{obs} derived empirically from the in vivo DDI data (i.e., for diltiazem; 0.01 minute^{-1} for HLMs and 0.006 minute^{-1} for HHEPs). In all cases, there were no instances of false negatives, and all positives were correctly identified. [Using the (b) criteria, this is obviously the case since the boundary was defined by the lowest k_{obs} value for a drug known to cause a DDI.] Thus, these assays are highly sensitive to classify molecules exhibiting in vitro TDI. However, the false positive rates translating k_{obs} directly to clinical DDI are as high as 40% when using the criteria of k_{obs} statistically different from solvent control and 28% when using the k_{obs} cutoff criteria. Thus, these assays, although sensitive, have unsatisfactory specificity. The highest positive predictive value was 65%, which was obtained using data from HHEPs and a k_{obs} cutoff value of 0.006 minute^{-1}. When using these assays in a prospective manner, as in early drug discovery, compounds not demonstrating TDI can be progressed with confidence that they will not cause DDI, but those demonstrating in vitro TDI may or may not cause DDI.

TABLE 2

Mean (S.E.) solvent control–subtracted in vitro k_{obs} in human liver microsomes and human hepatocytes. The within-experiment solvent control–subtracted k_{obs} is reported. The avg. HLM solvent control k_{obs} value was 0.0056 ± 0.0013 minute^{-1} (S.D.); the avg. HHEP solvent control k_{obs} value was −0.0010 ± 0.0031 minute^{-1} (S.D.)

Drug Name	HLM k_{obs} (min^{-1}) (S.E.)	HHEP k_{obs} (min^{-1}) (S.E.)
Terbinafine	−0.0010 (0.0013)	0.0008 (0.0011)
Atomoxetine	−0.0008 (0.0005)	0 (0.0004)
Flumazenil	−0.0006 (0.0002)	−0.0003 (0.0003)
Pimavanserin	−0.0004 (0.0005)	0.0009 (0.0002)*
Quetiapine	−0.0003 (0.0003)	0.0006 (0.0002)
Citalopram	−0.0001 (0.0004)	−0.0003 (0.0003)
Raltegravir	0 (0.0010)	0 (0.0002)
Ramelteon	0.0002 (0.0004)	0.0008 (0.0014)
Naltrexone	0.0005 (0.0004)	0.0003 (0.0002)
Fluoxetine	0.0011 (0.0006)	0.0011 (0.0002)*
Propranolol	0.0016 (0.0005)*	0 (0.0002)
Eplerenone	0.0018 (0.0003)*	0.0007 (0.0003)
Azithromycin	0.0018 (0.0004)*	0.0009 (0.0004)
Simvastatin	0.0029 (0.0005)*	−0.0002 (0.0008)
Sorafenib	0.0043 (0.0007)*	0.0015 (0.0009)
Terfenadine	0.0062 (0.0004)*	0.0025 (0.0008)*
Paroxetine	0.0083 (0.0007)*	0.0033 (0.0007)*
Diltiazem	0.0112 (0.0004)*	0.0060 (0.0012)*
Midostaurin	0.0131 (0.0005)*	0.0027 (0.0008)*
Propiverine	0.0153 (0.0011)*	0.0062 (0.0006)*
Nitrendipine	0.0166 (0.0004)*	0.0016 (0.0007)
Panobinostat	0.0175 (0.0015)*	0.0026 (0.0007)*
Amlodipine	0.0197 (0.0012)*	0.0249 (0.0037)*
Itraconazole[a]	0.0197 (0.0029)*	—
Imatinib	0.0235 (0.0022)*	0.0115 (0.0028)*
Erythromycin	0.0271 (0.0012)*	0.0118 (0.0026)*
Buspirone	0.0276 (0.0017)*	0.0059 (0.0014)*
Idelalisib	0.0312 (0.0011)*	—
Clarithromycin	0.0321 (0.0025)*	0.0074 (0.0014)*
Alectinib	0.0334 (0.0055)*	—
Verapamil	0.0374 (0.0013)*	0.0196 (0.003)*
Nilotinib[b]	0.0484 (0.0035)*	—
Carfilzomib	0.0626 (0.0017)*	0.0066 (0.0012)*
Tabimorelin	0.0662 (0.0074)*	0.0277 (0.0024)*
Saquinavir	0.0741 (0.0039)*	0.1742 (0.0447)*
Nefazodone	0.0754 (0.0015)*	0.0088 (0.0007)*
Telithromycin	0.0818 (0.0063)*	0.0342 (0.0021)*
Disulfiram	0.0865 (0.0028)*	0 (0.0008)
Tadalafil	0.0970 (0.0052)*	0.0078 (0.0007)*
Telaprevir	0.1037 (0.0073)*	0.0068 (0.0006)*
Troleandomycin	0.1166 (0.0055)*	0.2826 (0.0423)*
Conivaptan[c,d]	0.1293 (0.0144)*	0.0267 (0.0025)*
Ethinyl estradiol	0.1393 (0.0049)*	0.0052 (0.0011)*
Erlotinib[e]	0.1517 (0.0043)*	0.01037 (0.0024)*
Cobicistat[c,d]	0.1528 (0.0113)*	0.2174 (0.0599)*
Mibefradil[c,f]	0.1565 (0.0019)*	0.0045 (0.0015)*
Boceprevir	0.1737 (0.0062)*	0.0450 (0.0039)*
Tofisopam[c]	0.1926 (0.0071)*	—
Nelfinavir[c,d]	0.2187 (0.0019)*	0.0249 (0.0031)*
Ritonavir[g]	0.2333 (0.0027)*	—

[a]HLM test conc. 1 μM.
[b]HLM test conc. 10 μM.
[c]HLM test conc. 3 μM.
[d]HHEP test conc. 3 μM.
[e]HHEP test conc. 21 μM.
[f]HHEP test conc. 0.3 μM.
[g]HLM test conc. 0.3 μM.
*Signifies the $k_{obs,\ inhibitor}$ was statistically different from solvent control ($P < 0.05$); P values are shown in Supplemental Table 1.

Discussion

Drugs exhibiting time-dependent inhibition of CYP3A is one of the main causes of drug interactions by virtue of the large number of drugs for which CYP3A-catalyzed metabolism is the main clearance mechanism. Because so many drugs are cleared by CYP3A, it is desired that new drug candidates lack the ability to cause TDI for CYP3A. TDI assays are employed early in the drug research process, sometimes as one

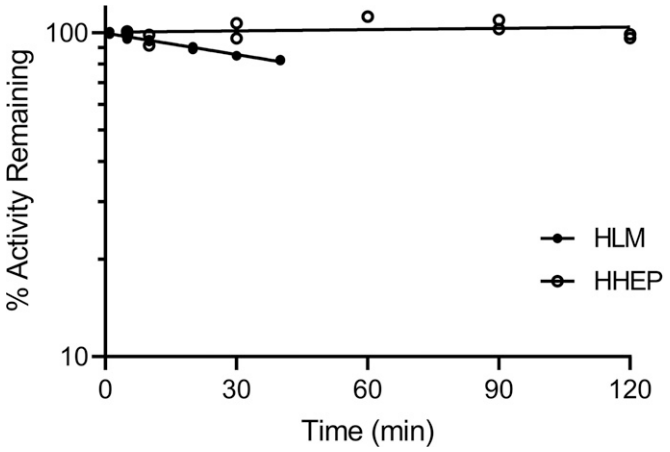

Fig. 2. Plot of representative solvent control percent activity remaining data. The regression of percent remaining activity versus time is shown for HLMs and HHEPs from representative solvent controls, in which the slopes represent $-k_{obs}$. Average solvent control k_{obs} values are 0.0056 ± 0.0014 minute^{-1} (range: 0.0040–0.0087 minute^{-1}) and −0.0010 ± 0.0030 minute^{-1} (range: −0.0072 to 0.0042 minute^{-1}) for HLMs and HHEPs, respectively. These studies were conducted $n = 2$.

of the earliest absorption, distribution, metabolism, and excretion assays performed along with other in vitro assays (e.g., metabolic lability, membrane permeability, etc.) that yield a fundamental knowledge of potential dispositional properties. Compounds exhibiting TDI for CYP3A are undesired, and early TDI data are used either in a simple binary filter fashion, or they are used to develop structure-activity relationships to aid medicinal chemists in the design of alternate compounds that lack this property. However, we and others (Zimmerlin et al., 2011) have observed generally high hit rates in CYP3A TDI assays using HLMs, and frequently the compounds exhibiting TDI possess none of the well known structural entities that have been associated with mechanism-based inactivation of cytochrome P450 enzymes (Orr et al., 2012; Kalgutkar, 2017). Furthermore, utilization of CYP3A in vitro TDI parameters (k_{inact}/K_I) generated in HLMs in DDI prediction algorithms frequently led to overestimations of in vivo DDI (Rowland Yeo et al., 2011; Vieira et al., 2014). This leaves drug design teams with the ambiguity of whether the CYP3A TDI data generated is relevant to clinical DDI for their newly synthesized compounds and useful in decision-making of compound progression or for use in development of structure-activity relationships. Thus, the objective of the present study was to address three questions: 1) Do drugs that do not cause DDI with CYP3A yield measurable TDI data in HLM?; 2) If so, is there an empirical boundary line for in vitro TDI values under which the TDI data can be disregarded as an important design attribute?; and 3) Is there a difference in this relationship for TDI data generated in human liver microsomes versus human hepatocytes?

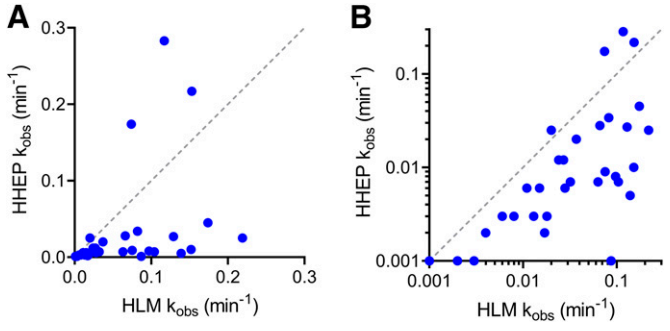

Fig. 3. Plot of HHEP versus HLM k_{obs}. k_{obs} was evaluated for 43 drugs at the same test concentration in both HLMs and HHEPs. (A) shows data on linear-scaled axes wherein the dashed line is the line of unity, and (B) shows data on log-log scaled axes. The three drugs for which HHEP k_{obs} is greater than HLM k_{obs} are saquinavir, troleandomycin, and cobicistat. A single k_{obs} determination was done for each drug.

In HLMs, the drugs evaluated in this study can be considered in three groups: 1) those that demonstrate a measurable k_{obs} values and are known to cause a DDI (e.g., clarithromycin, verapamil, etc.), 2) drugs that show no detectable k_{obs} (i.e., no statistical difference from solvent control) and also did not cause a DDI for a CYP3A-cleared drug (e.g., fluoxetine, terbinafine), and 3) drugs that show measurable and statistically significant k_{obs} values but do not cause a meaningful DDI (AUCR < 2) on a CYP3A-cleared drug (e.g., propranolol, paroxetine, erlotinib) (Fig. 4A). The latter group can be considered false positives; TDI is observed in vitro but DDI is not observed in vivo (Fig. 5). It is certainly the case that there are other very important considerations when attempting to relate in vitro TDI data to in vivo DDI, most important being the dose and exposure of the time-dependent inhibitor. However, in early drug research efforts, the potential dose that will be needed for efficacy is not yet known, and accordingly, design teams are faced with uncertainty when new compounds exhibit TDI. Thus, using the set of drugs in this study, boundary lines for k_{obs} values were established for decision-making. For HLMs, a k_{obs} value of 0.01 minute^{-1} was established as a boundary under which there are no drugs known to cause a clinical DDI with a CYP3A-cleared drug. Thus, even when k_{obs} values can be statistically different from solvent control, these compounds are highly unlikely to be of any concern for a DDI liability. Above this cutoff value, there are still many drugs that do not cause a clinical DDI, whereas others do. Drug design teams can continue to pursue compounds in this category, but the risk of ultimately pursuing a compound that will cause DDI is greater, especially if the dose ultimately needed for clinical efficacy is high.

Although cytochrome P450 TDI assays are well established in HLMs, reports have been emerging on the use of suspended HHEPs for this measurement (Zhao et al., 2005; Xu et al., 2009; Chen et al., 2011; Mao et al., 2011, 2012, 2013, 2016; Kimoto et al., 2019). Thus, an evaluation was undertaken in which nearly the same set of drugs were tested as TDI in HHEP suspension assays. It was noteworthy that with the exception of three drugs, the k_{obs} values in hepatocytes were much lower than those in liver microsomes (Fig. 3). Interestingly, the relationship did not exhibit a simple linear shift, which is indicative that the difference in TDI observed in HLMs versus HHEPs is unlikely to be related to a single mechanism. The statistical difference from solvent control was observable at lower k_{obs} values because the rate of loss of CYP3A activity in hepatocytes was much slower than that for liver microsomes (Fig. 2). The same interrogation of the data for cutoff boundaries was done for the hepatocyte data, and a similar observation could be made as for microsomes (Fig. 4B), albeit the absolute value for the boundary line was lower for hepatocytes than that for microsomes. Hepatocytes offer additional complexity that may better represent the actual in vivo situation relative to liver microsomes. Reactive intermediates generated by CYP3A that may be the cause of TDI in liver microsomes could be quenched by further metabolism by conjugating enzymes active in hepatocytes (e.g., glutathione transferase, glucuronosyl transferase, and others) but absent in microsomes. In hepatocytes, there is a membrane barrier between the medium to which the test compound is dosed and the cytochrome P450 enzymes inside the cells, and test compounds that have low membrane permeability could be expected to cause lower inactivation rates. Other unknown mechanisms could be operating in the intact cellular milieu that protect CYP3A from inactivation that are not operative in liver microsomes. Currently, a reason for the differences

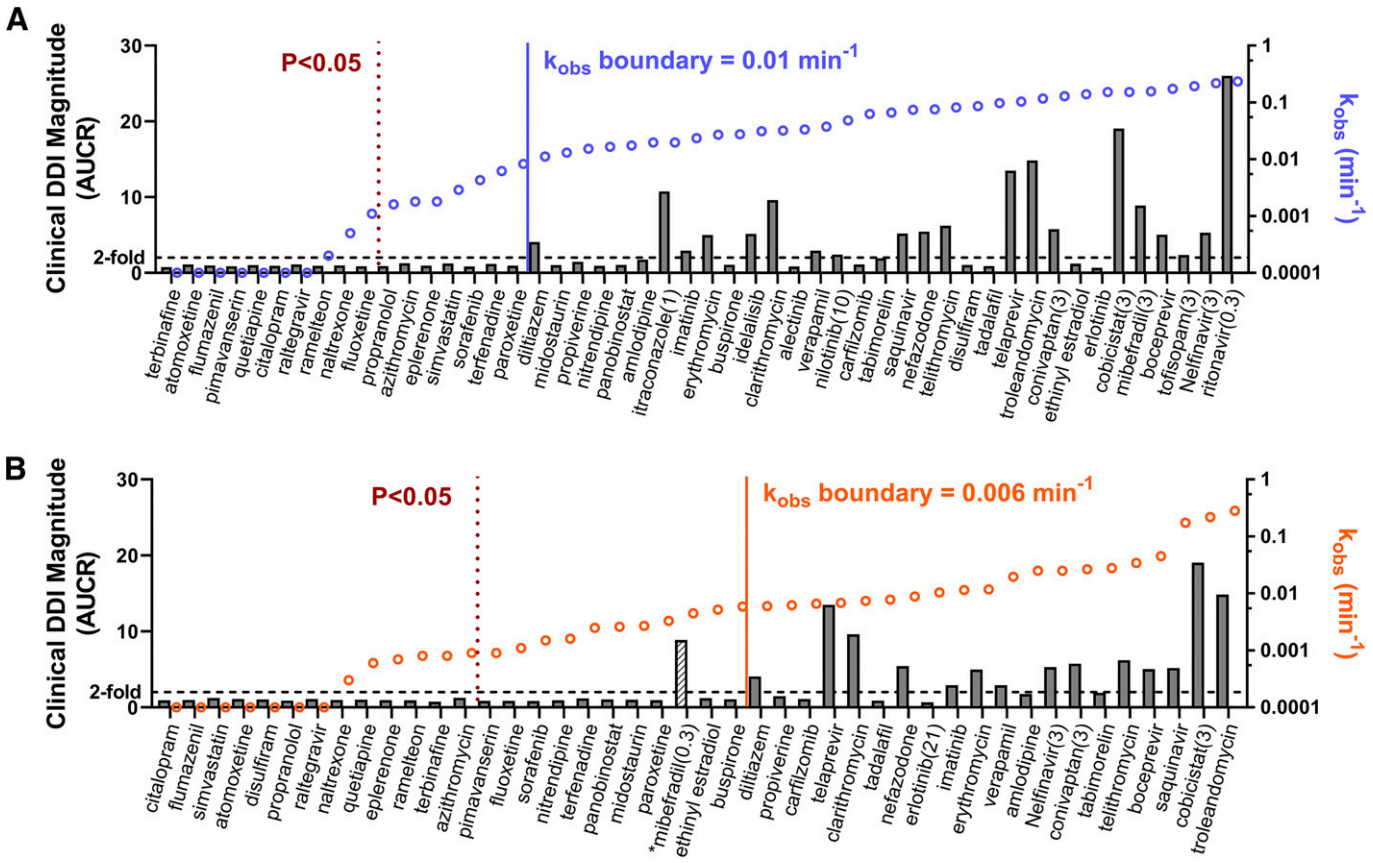

Fig. 4. Boundary line for k_{obs} associated with DDI as measured in HLMs and HHEPs. (A) Fifty drugs were evaluated for CYP3A TDI in human liver microsomes at 30 μM (unless otherwise noted in parentheses) and ranked in order of increasing k_{obs}. The gray bars represent the observed clinical DDI magnitude and are plotted against the left *y*-axis. The hollow blue circles represent the k_{obs} (solvent control–subtracted) and are plotted against the right *y*-axis. This established the 0.01 minute^{-1} k_{obs} boundary at which ≥2-fold clinical interactions were observed, represented by the vertical blue line. The dotted red line represents the k_{obs} boundary at which in vitro statistical significance ($P < 0.05$) was achieved. (B) Forty-four drugs were evaluated for CYP3A TDI in human hepatocytes at 30 μM (unless otherwise noted in parentheses) and ranked in order of increasing k_{obs}. The gray bars represent the observed clinical DDI magnitude and are plotted against the left *y*-axis. The hollow orange circles represent the k_{obs} (solvent control–subtracted) and are plotted against the right *y*-axis. This established the 0.006 minute^{-1} k_{obs} boundary at which ≥2-fold clinical interactions were observed, represented by the vertical orange line. The dotted red line represents the kobs boundary at which in vitro statistical significance ($P < 0.05$) was achieved. *Mibefradil k_{obs} had to be measured at 0.3 μM and therefore was not used to define the boundary line for drugs tested at 30 μM. A single k_{obs} determination was done for each drug.

between TDI data generated in microsomes and hepatocytes is unknown.

Overall, generation of this in vitro TDI dataset with drugs that have been evaluated for CYP3A DDI in the clinic has shown that many drugs will exhibit TDI in vitro but show no clinically meaningful DDI in vivo. In some instances, this may be because the clinical dose given and/or free exposure is low (e.g., ethinyl estradiol), but in others the reason is unknown. Boundaries are established such that when below a k_{obs} value (at a test concentration of 30 μM generally used in this investigation) there is little concern that the test compound will be a perpetrator of a clinically meaningful DDI, even when the rate of loss in CYP3A activity is statistically distinguishable from the solvent control. Furthermore, when a test compound demonstrates a k_{obs} value above the boundary it does not necessarily mean that the compound will cause DDI, only that the likelihood of this is greater. The boundary k_{obs} values reported here, 0.01 minute^{-1} for liver microsomes and 0.006 minute^{-1} for suspended hepatocytes, were determined for the pooled lots used in this investigation. Specific values may vary with different preparations. Such simple boundaries can be of use when TDI data are generated early in a drug research process and decisions need to be made regarding whether the TDI data need to be taken seriously or whether the risk of DDI may be exaggerated. This can be used in conjunction with knowledge of the chemical structure (i.e., whether the compound showing TDI possesses a structure known to cause TDI) as well as follow-up experiments to uncover a mechanism for the TDI (e.g., bioactivation to reactive intermediates, generation of a metabolite-intermediate complex, adduction to protein or heme) (Hollenberg et al., 2008; Orr et al., 2012). These latter experiments can confirm the kinetic observation of TDI with mechanistic evidence.

	True Positive	False Negative
	False Positive	True Negative

	HLM		HHEP	
P-value	k_{obs} P < 0.05	k_{obs} P ≥ 0.05	k_{obs} P < 0.05	k_{obs} P ≥ 0.05
AUCR ≥ 2	20 (40%)	0 (0%)	15 (34%)	0 (0%)
AUCR < 2	20 (40%)	10 (20%)	16 (36%)	13 (30%)
Positive Predictive Value:	50%		48%	
Boundary	k_{obs} ≥ 0.01 min^{-1}	k_{obs} < 0.01 min^{-1}	k_{obs} ≥ 0.006 min^{-1}	k_{obs} < 0.006 min^{-1}
AUCR ≥ 2	20 (40%)	0 (0%)	15 (34%)	0 (0%)
AUCR < 2	13 (26%)	17 (34%)	8 (18%)	21 (48%)
Positive Predictive Value:	61%		65%	

Fig. 5. Classification tables of measured k_{obs} in HLMs and HHEPs compared with observed DDI. A summary of diagnostic test results is presented. Classifications are shown for k_{obs} measured in HLMs or HHEPs using either a k_{obs} statistical parallel lines test ($P < 0.05$) or boundary criteria compared against the observed DDI. Values are displayed as both count and percent of total ($n = 50$ for HLMs, $n = 44$ for HHEPs).

It is important to note that these experiments were designed with early drug research decision-making processes in mind. For these purposes, we considered a clinical DDI magnitude of 2-fold to be relevant for decision-making at this point. Most pharmacotherapies can withstand 2-fold changes in exposure without deleterious outcomes, and it is only for those drugs with extremely narrow therapeutic indices (e.g., alfentanyl, cisapride, cyclosporine, fentanyl, terfenadine, quinidine, or tacrolimus) in which a doubling of exposure can be harmful. This is consistent with current regulatory guidance regarding the preferred approach to define no-effect DDI boundaries for substrate drugs, which should be based on concentration-response relationships derived from pharmacokinetic and pharmacodynamic analyses as well as other information, such as the maximum-tolerated dose (Food and Drug Administration, 2020). In contrast, when no-effect boundaries are not clearly defined by the former approach, drug regulatory agencies define increases in exposure of a mere 1.25-fold to be a cutoff for DDI, which is recognized as a very conservative standard for drugs that have wide safety margins. Nevertheless, in early drug research, multiple parameters and properties undergo simultaneous optimization (e.g., potency, clearance, and oral absorption), which is a difficult task, and thus driving drug design to avoid nominal DDIs (i.e., 1.25–2.0-fold) is of lower priority. As drug candidates progress into the development phase, more elaborate TDI experiments (e.g., K_I/k_{inact}) can be done to generate the data needed for projecting clinical DDI through physiologically based pharmacokinetic modeling, and through this process, more refined predictions can be made and include more subtle DDIs. The reported findings of the present work must be viewed as for the purposes of defining simple cutoff values for early decision-making.

In summary, this report established that many drugs that do not cause DDI with CYP3A yield measurable TDI data in human liver microsomes and hepatocytes. Empirical boundary lines for in vitro TDI values under which the TDI data can be disregarded as an important design attribute were established, with approximately 1.7-fold–lower boundary conditions in hepatocytes relative to liver microsomes. Future endeavors of this research include understanding why the different values are observed between liver microsomes and hepatocytes, why some compounds show TDI without possessing one of the known structural elements associated with this phenomenon, and how TDI data can be better used in predicting clinical DDI.

Acknowledgments

The authors would like to thank Lauren Horlbogen for conducting several in vitro studies.

Authorship Contributions

Participated in research design: Eng, Tseng, Cerny, Goosen, Obach.

Conducted experiments: Eng, Tseng.

Performed data analysis: Eng, Tseng, Cerny, Obach.

Wrote or contributed to the writing of the manuscript: Eng, Tseng, Cerny, Goosen, Obach.

References

Adams M, Pieniaszek HJ Jr., Gammaitoni AR, and Ahdieh H (2005) Oxymorphone extended release does not affect CYP2C9 or CYP3A4 metabolic pathways. *J Clin Pharmacol* **45**:337–345.

Ahonen J, Olkkola KT, and Neuvonen PJ (1995) Effect of itraconazole and terbinafine on the pharmacokinetics and pharmacodynamics of midazolam in healthy volunteers. *Br J Clin Pharmacol* **40**:270–272.

Backman JT, Olkkola KT, Aranko K, Himberg JJ, and Neuvonen PJ (1994) Dose of midazolam should be reduced during diltiazem and verapamil treatments. *Br J Clin Pharmacol* **37**:221–225.

Baer BR, Wienkers LC, and Rock DA (2007) Time-dependent inactivation of P450 3A4 by raloxifene: identification of Cys239 as the site of apoprotein alkylation. *Chem Res Toxicol* **20**: 954–964.

Barbara JE, Kazmi F, Parkinson A, and Buckley DB (2013) Metabolism-dependent inhibition of CYP3A4 by lapatinib: evidence for formation of a metabolic intermediate complex with a nitroso/oxime metabolite formed via a nitrone intermediate. *Drug Metab Dispos* **41**:1012–1022.

Becquemont L, Neuvonen M, Verstuyft C, Jaillon P, Letierce A, Neuvonen PJ, and Funck-Brentano C (2007) Amiodarone interacts with simvastatin but not with pravastatin disposition kinetics. *Clin Pharmacol Ther* **81**:679–684.

Buch AB, Van Harken DR, Seidehamel RJ, and Barbhaiya RH (1993) A study of pharmacokinetic interaction between buspirone and alprazolam at steady state. *J Clin Pharmacol* **33**:1104–1109.

Calvert H, Twelves C, Ranson M, Plummer R, Fettner S, Pantze M, Ling J, Hamilton M, Lum BL, and Rakhit A (2014) Effect of erlotinib on CYP3A activity, evaluated in vitro and by dual probes in patients with cancer. *Anticancer Drugs* **25**:832–840.

Carls A, Jedamzik J, Witt L, Hohmann N, Burhenne J, and Mikus G (2014) Systemic exposure of topical erythromycin in comparison to oral administration and the effect on cytochrome P450 3A4 activity. *Br J Clin Pharmacol* **78**:1433–1440.

Chen Y, Liu L, Monshouwer M, and Fretland AJ (2011) Determination of time-dependent inactivation of CYP3A4 in cryopreserved human hepatocytes and assessment of human drug-drug interactions. *Drug Metab Dispos* **39**:2085–2092.

Cook CS, Berry LM, and Burton E (2004) Prediction of in vivo drug interactions with eplerenone in man from in vitro metabolic inhibition data. *Xenobiotica* **34**:215–228.

Dutreix C, Munarini F, Lorenzo S, Roesel J, and Wang Y (2013) Investigation into CYP3A4-mediated drug-drug interactions on midostaurin in healthy volunteers. *Cancer Chemother Pharmacol* **72**:1223–1234.

Einolf HJ (2007) Comparison of different approaches to predict metabolic drug-drug interactions. *Xenobiotica* **37**:1257–1294.

Einolf HJ, Lin W, Won CS, Wang L, Gu H, Chun DY, He H, and Mangold JB (2017) Physiologically based pharmacokinetic model predictions of panobinostat (LBH589) as a victim and perpetrator of drug-drug interactions. *Drug Metab Dispos* **45**:1304–1316.

Food and Drug Administration (2004) Drug approval package: Ketek (telithromycin). FDA application NDA 021144. Food and Drug Administration, Silver Springs, MD.

Food and Drug Administration (2005a) Drug approval package: Rozerem (ramelteon). FDA application NDA 021782. Food and Drug Administration, Silver Springs, MD.

Food and Drug Administration (2005b) Drug approval package: Vaprisol (conivaptan). FDA application NDA 021697. Food and Drug Administration, Silver Springs, MD.

Food and Drug Administration (2011) Drug approval package: Victrelis (boceprevir). FDA application NDA 202258. Food and Drug Administration, Silver Springs, MD.

Food and Drug Administration (2016) Drug approval package: Nuplazid (pimavanserin tartrate). FDA application NDA 207318. Food and Drug Administration, Silver Springs, MD.

Food and Drug Administration (2020) Clinical drug interaction studies - cytochrome P450 enzyme- and transporter-mediated drug interactions guidance for industry. *Center for Drug Evaluation and Research (CDER), US Department of Health and Human Services Food and Drug Administration, Silver Springs, MD.*

Filppula AM, Parvizi R, Mateus A, Baranczewski P, and Artursson P (2019) Improved predictions of time-dependent drug-drug interactions by determination of cytosolic drug concentrations. *Sci Rep* **9**:5850.

Flaherty KT, Lathia C, Frye RF, Schuchter L, Redlinger M, Rosen M, and O'Dwyer PJ (2011) Interaction of sorafenib and cytochrome P450 isoenzymes in patients with advanced melanoma: a phase I/II pharmacokinetic interaction study. *Cancer Chemother Pharmacol* **68**:1111–1118.

Franklin MR (1977) Inhibition of mixed-function oxidations by substrates forming reduced cytochrome P-450 metabolic-intermediate complexes. *Pharmacol Ther A* **2**:227–245.

Friedman EJ, Fraser IP, Wang YH, Bergman AJ, Li CC, Larson PJ, Chodakewitz J, Wagner JA, and Stoch SA (2011) Effect of different durations and formulations of diltiazem on the single-dose pharmacokinetics of midazolam: how long do we go? *J Clin Pharmacol* **51**:1561–1570.

Friedman H, Greenblatt DJ, Burstein ES, Scavone JM, Harmatz JS, and Shader RI (1988) Triazolam kinetics: interaction with cimetidine, propranolol, and the combination. *J Clin Pharmacol* **28**:228–233.

Garg V, Chandorkar G, Farmer HF, Smith F, Alves K, and van Heeswijk RP (2012) Effect of telaprevir on the pharmacokinetics of midazolam and digoxin. *J Clin Pharmacol* **52**:1566–1573.

Gorski JC, Hall SD, Jones DR, VandenBranden M, and Wrighton SA (1994) Regioselective biotransformation of midazolam by members of the human cytochrome P450 3A (CYP3A) subfamily. *Biochem Pharmacol* **47**:1643–1653.

Gorski JC, Jones DR, Haehner-Daniels BD, Hamman MA, O'Mara EM Jr., and Hall SD (1998) The contribution of intestinal and hepatic CYP3A to the interaction between midazolam and clarithromycin. *Clin Pharmacol Ther* **64**:133–143.

Greenblatt DJ, Peters DE, Oleson LE, Harmatz JS, MacNab MW, Berkowitz N, Zinny MA, and Court MH (2009) Inhibition of oral midazolam clearance by boosting doses of ritonavir, and by 4,4-dimethyl-benziso-(2H)-selenazine (ALT-2074), an experimental catalytic mimic of glutathione oxidase. *Br J Clin Pharmacol* **68**:920–927.

Grimm SW, Einolf HJ, Hall SD, He K, Lim HK, Ling KH, Lu C, Nomeir AA, Seibert E, Skordos KW, et al. (2009) The conduct of in vitro studies to address time-dependent inhibition of drug-metabolizing enzymes: a perspective of the pharmaceutical research and manufacturers of America. *Drug Metab Dispos* **37**:1355–1370.

Handel J, Ziegler G, Gemeinhardt A, Stuber H, Fischer C, and Klotz U (1988) Lack of effect of nitrendipine on the pharmacokinetics and pharmacodynamics of midazolam during steady state. *Br J Clin Pharmacol* **25**:243–250.

Hollenberg PF, Kent UM, and Bumpus NN (2008) Mechanism-based inactivation of human cytochromes p450s: experimental characterization, reactive intermediates, and clinical implications. *Chem Res Toxicol* **21**:189–205.

Iwamoto M, Kassahun K, Troyer MD, Hanley WD, Lu P, Rhoton A, Petry AS, Ghosh K, Mangin E, DeNoia EP, et al. (2008) Lack of a pharmacokinetic effect of raltegravir on midazolam: in vitro/in vivo correlation. *J Clin Pharmacol* **48**:209–214.

Jin F, Robeson M, Zhou H, Moyer C, Wilbert S, Murray B, and Ramanathan S (2015) Clinical drug interaction profile of idelalisib in healthy subjects. *J Clin Pharmacol* **55**:909–919.

Jones H and Rowland-Yeo K (2013) Basic concepts in physiologically based pharmacokinetic modeling in drug discovery and development. *CPT Pharmacometrics Syst Pharmacol* **2**:e63.

Kalgutkar AS (2017) Liabilities associated with the formation of "hard" electrophiles in reactive metabolite trapping screens. *Chem Res Toxicol* **30**:220–238.

Kawano S, Kamataki T, Yasumori T, Yamazoe Y, and Kato R (1987) Purification of human liver cytochrome P-450 catalyzing testosterone 6 beta-hydroxylation. *J Biochem* **102**:493–501.

Kenny JR, Mukadam S, Zhang C, Tay S, Collins C, Galetin A, and Khojasteh SC (2012) Drug-drug interaction potential of marketed oncology drugs: in vitro assessment of time-dependent cytochrome P450 inhibition, reactive metabolite formation and drug-drug interaction prediction. *Pharm Res* **29**:1960–1976.

Kharasch ED, Hankins DC, Jubert C, Thummel KE, and Taraday JK (1999) Lack of single-dose disulfiram effects on cytochrome P-450 2C9, 2C19, 2D6, and 3A4 activities: evidence for specificity toward P-450 2E1. *Drug Metab Dispos* **27**:717–723.

Kharasch ED, Hoffer C, Whittington D, Walker A, and Bedynek PS (2009) Methadone pharmacokinetics are independent of cytochrome P4503A (CYP3A) activity and gastrointestinal drug transport: insights from methadone interactions with ritonavir/indinavir. *Anesthesiology* **110**: 660–672.

Kharasch ED, Walker A, Hoffer C, and Sheffels P (2004) Intravenous and oral alfentanil as in vivo probes for hepatic and first-pass cytochrome P450 3A activity: noninvasive assessment by use of pupillary miosis. *Clin Pharmacol Ther* **76**:452–466.

Khazaal Y, Preisig M, Chatton A, Kaufmann N, Bilancioni R, and Eap CB (2013) Use of high doses of quetiapine in bipolar disorder episodes are not linked to high activity of cytochrome P4503A4 and/or cytochrome P4502D6. *Psychiatr Q* **84**:329–335.

Kimoto E, Vourvahis M, Scialis RJ, Eng H, Rodrigues AD, and Varma MVS (2019) Mechanistic evaluation of the complex drug-drug interactions of maraviroc: contribution of cytochrome P450 3A, P-glycoprotein and organic anion transporting polypeptide 1B1. *Drug Metab Dispos* **47**:493–503.

Kirby BJ, Collier AC, Kharasch ED, Whittington D, Thummel KE, and Unadkat JD (2011) Complex drug interactions of HIV protease inhibitors 1: inactivation, induction, and inhibition of cytochrome P450 3A by ritonavir or nelfinavir. *Drug Metab Dispos* **39**:1070–1078.

Kivistö KT, Lamberg TS, Kantola T, and Neuvonen PJ (1997) Plasma buspirone concentrations are greatly increased by erythromycin and itraconazole. *Clin Pharmacol Ther* **62**:348–354.

Kokudai M, Inui N, Takeuchi K, Sakaeda T, Kagawa Y, and Watanabe H (2009) Effects of statins on the pharmacokinetics of midazolam in healthy volunteers. *J Clin Pharmacol* **49**:568–573.

Lam YW, Alfaro CL, Ereshefsky L, and Miller M (2003) Pharmacokinetic and pharmacodynamic interactions of oral midazolam with ketoconazole, fluoxetine, fluvoxamine, and nefazodone. *J Clin Pharmacol* **43**:1274–1282.

Lamberg TS, Kivistö KT, and Neuvonen PJ (1999) Lack of effect of terfenadine on the pharmacokinetics of the CYP3A4 substrate buspirone. *Pharmacol Toxicol* **84**:165–169.

Lin HL, Kent UM, and Hollenberg PF (2002) Mechanism-based inactivation of cytochrome P450 3A4 by 17 alpha-ethynylestradiol: evidence for heme destruction and covalent binding to protein. *J Pharmacol Exp Ther* **301**:160–167.

Mao J, Johnson TR, Shen Z, and Yamazaki S (2013) Prediction of crizotinib-midazolam interaction using the Simcyp population-based simulator: comparison of CYP3A time-dependent inhibition between human liver microsomes versus hepatocytes. *Drug Metab Dispos* **41**:343–352.

Mao J, Mohutsky MA, Harrelson JP, Wrighton SA, and Hall SD (2011) Prediction of CYP3A-mediated drug-drug interactions using human hepatocytes suspended in human plasma. *Drug Metab Dispos* **39**:591–602.

Mao J, Mohutsky MA, Harrelson JP, Wrighton SA, and Hall SD (2012) Predictions of cytochrome P450-mediated drug-drug interactions using cryopreserved human hepatocytes: comparison of plasma and protein-free media incubation conditions. *Drug Metab Dispos* **40**:706–716.

Mao J, Tay S, Khojasteh CS, Chen Y, Hop CE, and Kenny JR (2016) Evaluation of time dependent inhibition assays for marketed oncology drugs: comparison of human hepatocytes and liver microsomes in the presence and absence of human plasma. *Pharm Res* **33**:1204–1219.

Martin DE, Zussman BD, Everitt DE, Benincosa LJ, Etheredge RC, and Jorkasky DK (1997) Paroxetine does not affect the cardiac safety and pharmacokinetics of terfenadine in healthy adult men. *J Clin Psychopharmacol* **17**:451–459.

Mathias AA, German P, Murray BP, Wei L, Jain A, West S, Warren D, Hui J, and Kearney BP (2010) Pharmacokinetics and pharmacodynamics of GS-9350: a novel pharmacokinetic enhancer without anti-HIV activity. *Clin Pharmacol Ther* **87**:322–329.

McConn DJ II, Lin YS, Allen K, Kunze KL, and Thummel KE (2004) Differences in the inhibition of cytochromes P450 3A4 and 3A5 by metabolite-inhibitor complex-forming drugs. *Drug Metab Dispos* **32**:1083–1091.

Morcos PN, Cleary Y, Guerini E, Dall G, Bogman K, De Petris L, Viteri S, Bordogna W, Yu L, Martin-Facklam M, et al. (2017) Clinical drug-drug interactions through cytochrome P450 3A (CYP3A) for the selective ALK inhibitor alectinib. *Clin Pharmacol Drug Dev* **6**:280–291.

Nolting A and Abramowitz W (2000) Lack of interaction between citalopram and the CYP3A4 substrate triazolam. *Pharmacotherapy* **20**:750–755.

Obach RS, Walsky RL, and Venkatakrishnan K (2007) Mechanism-based inactivation of human cytochrome p450 enzymes and the prediction of drug-drug interactions. *Drug Metab Dispos* **35**: 246–255.

Obach RS, Walsky RL, Venkatakrishnan K, Gaman EA, Houston JB, and Tremaine LM (2006) The utility of in vitro cytochrome P450 inhibition data in the prediction of drug-drug interactions. *J Pharmacol Exp Ther* **316**:336–348.

O'Brien SG, Meinhardt P, Bond E, Beck J, Peng B, Dutreix C, Mehring G, Milosavljev S, Huber C, Capdeville R, et al. (2003) Effects of imatinib mesylate (STI571, Glivec) on the pharmacokinetics of simvastatin, a cytochrome p450 3A4 substrate, in patients with chronic myeloid leukaemia. *Br J Cancer* **89**:1855–1859.

Olkkola KT, Backman JT, and Neuvonen PJ (1994) Midazolam should be avoided in patients receiving the systemic antimycotics ketoconazole or itraconazole. *Clin Pharmacol Ther* **55**:481–485.

Orr ST, Ripp SL, Ballard TE, Henderson JL, Scott DO, Obach RS, Sun H, and Kalgutkar AS (2012) Mechanism-based inactivation (MBI) of cytochrome P450 enzymes: structure-activity relationships and discovery strategies to mitigate drug-drug interaction risks. *J Med Chem* **55**: 4896–4933.

Palkama VJ, Ahonen J, Neuvonen PJ, and Olkkola KT (1999) Effect of saquinavir on the pharmacokinetics and pharmacodynamics of oral and intravenous midazolam. *Clin Pharmacol Ther* **66**: 33–39.

Palovaara S, Kivistö KT, Tapanainen P, Manninen P, Neuvonen PJ, and Laine K (2000) Effect of an oral contraceptive preparation containing ethinylestradiol and gestodene on CYP3A4 activity as measured by midazolam 1′-hydroxylation. *Br J Clin Pharmacol* **50**:333–337.

Raeder JC, Nilsen OG, and Hole A (1988) Pharmacokinetics of midazolam and alfentanil in outpatient general anesthesia. A study with concomitant thiopentone, flumazenil or placebo administration. *Acta Anaesthesiol Scand* **32**:467–472.

Ring BJ, Patterson BE, Mitchell MI, Vandenbranden M, Gillespie J, Bedding AW, Jewell H, Payne CD, Forgue ST, Eckstein J, et al. (2005) Effect of tadalafil on cytochrome P450 3A4-mediated clearance: studies in vitro and in vivo. *Clin Pharmacol Ther* **77**:63–75.

Rock BM, Hengel SM, Rock DA, Wienkers LC, and Kunze KL (2014) Characterization of ritonavir-mediated inactivation of cytochrome P450 3A4. *Mol Pharmacol* **86**:665–674.

Rogers JF, Morrison AL, Nafziger AN, Jones CL, Rocci ML Jr., and Bertino JS Jr. (2002) Flumazenil reduces midazolam-induced cognitive impairment without altering pharmacokinetics. *Clin Pharmacol Ther* **72**:711–717.

Rowland M and Matin SB (1973) Kinetics of drug-drug interactions. *J Pharmacokinet Biopharm* **1**:553–567.

Rowland Yeo K, Walsky RL, Jamei M, Rostami-Hodjegan A, and Tucker GT (2011) Prediction of time-dependent CYP3A4 drug-drug interactions by physiologically based pharmacokinetic modelling: impact of inactivation parameters and enzyme turnover. *Eur J Pharm Sci* **43**: 160–173.

Sauer JM, Long AJ, Ring B, Gillespie JS, Sanburn NP, DeSante KA, Petullo D, VandenBranden MR, Jensen CB, Wrighton SA, et al. (2004) Atomoxetine hydrochloride: clinical drug-drug interaction prediction and outcome. *J Pharmacol Exp Ther* **308**:410–418.

Tomalik-Scharte D, Jetter A, Kinzig-Schippers M, Skott A, Sörgel F, Klaassen T, Kasel D, Harlfinger S, Doroshyenko O, Frank D, et al. (2005) Effect of propiverine on cytochrome P450 enzymes: a cocktail interaction study in healthy volunteers. *Drug Metab Dispos* **33**:1859–1866.

Tóth M, Drabant S, Varga B, Végso G, Cseh A, Szentpéteri I, and Klebovich I (2008) Tofisopam inhibits the pharmacokinetics of CYP3A4 substrate midazolam. *Eur J Clin Pharmacol* **64**:93–94.

Veronese ML, Gillen LP, Dorval EP, Hauck WW, Waldman SA, and Greenberg HE (2003) Effect of mibefradil on CYP3A4 in vivo. *J Clin Pharmacol* **43**:1091–1100.

Vieira ML, Kirby B, Ragueneau-Majlessi I, Galetin A, Chien JY, Einolf HJ, Fahmi OA, Fischer V, Fretland A, Grime K, et al. (2014) Evaluation of various static in vitro-in vivo extrapolation models for risk assessment of the CYP3A inhibition potential of an investigational drug. *Clin Pharmacol Ther* **95**:189–198.

Wang YH, Jones DR, and Hall SD (2005) Differential mechanism-based inhibition of CYP3A4 and CYP3A5 by verapamil. *Drug Metab Dispos* **33**:664–671.

Wang Z, Yang J, Kirk C, Fang Y, Alsina M, Badros A, Papadopoulos K, Wong A, Woo T, Bomba D, et al. (2013) Clinical pharmacokinetics, metabolism, and drug-drug interaction of carfilzomib. *Drug Metab Dispos* **41**:230–237.

Waxman DJ, Attisano C, Guengerich FP, and Lapenson DP (1988) Human liver microsomal steroid metabolism: identification of the major microsomal steroid hormone 6 beta-hydroxylase cytochrome P-450 enzyme. *Arch Biochem Biophys* **263**:424–436.

Xu L, Chen Y, Pan Y, Skiles GL, and Shou M (2009) Prediction of human drug-drug interactions from time-dependent inactivation of CYP3A4 in primary hepatocytes using a population-based simulator. *Drug Metab Dispos* **37**:2330–2339.

Yates P, Eng H, Di L, and Obach RS (2012) Statistical methods for analysis of time-dependent inhibition of cytochrome p450 enzymes. *Drug Metab Dispos* **40**:2289–2296.

Zdravkovic M, Olsen AK, Christiansen T, Schulz R, Taub ME, Thomsen MS, Rasmussen MH, and Ilondo MM (2003) A clinical study investigating the pharmacokinetic interaction between NN703 (tabimorelin), a potential inhibitor of CYP3A4 activity, and midazolam, a CYP3A4 substrate. *Eur J Clin Pharmacol* **58**:683–688.

Zhang H, Sheng J, Ko JH, Zheng C, Zhou W, Priess P, Lin W, and Novick S (2015) Inhibitory effect of single and repeated doses of nilotinib on the pharmacokinetics of CYP3A substrate midazolam. *J Clin Pharmacol* **55**:401–408.

Zhao P, Kunze KL, and Lee CA (2005) Evaluation of time-dependent inactivation of CYP3A in cryopreserved human hepatocytes. *Drug Metab Dispos* **33**:853–861.

Zimmerlin A, Trunzer M, and Faller B (2011) CYP3A time-dependent inhibition risk assessment validated with 400 reference drugs. *Drug Metab Dispos* **39**:1039–1046.

Zimmermann T, Yeates RA, Laufen H, Scharpf F, Leitold M, and Wildfeuer A (1996) Influence of the antibiotics erythromycin and azithromycin on the pharmacokinetics and pharmacodynamics of midazolam. *Arzneimittelforschung* **46**:213–217.

Address correspondence to: Heather Eng, Pfizer Inc., Eastern Point Rd., Groton, CT 06340. E-mail: heather.eng@pfizer.com; or R. Scott Obach, Pfizer Inc., Eastern Point Rd., Groton, CT 06340. E-mail: r.scott.obach@pfizer.com